

AD-A161 091

QUANTUM MONTE CARLO FOR MOLECULES(U) CALIFORNIA UNIV
BERKELEY LAWRENCE BERKELEY LAB W A LESTER ET AL
01 NOV 85 N00014-83-F-0101

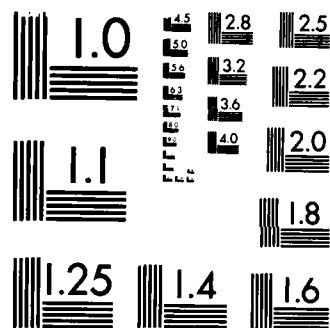
1/1

UNCLASSIFIED

F/G 20/10

NL

							END						
							FILMED						
							etc						



MICROCOPY RESOLUTION TEST CHART
NATIONAL BUREAU OF STANDARDS-1963-A

Unclassified

SECURITY CLASSIFICATION OF THIS PAGE (When Data Entered)

12

AD-A161 091

REPORT DOCUMENTATION PAGE		READ INSTRUCTIONS BEFORE COMPLETING FORM
1. REPORT NUMBER	2. GOVT ACCESSION NO.	3. RECIPIENT'S CATALOG NUMBER
	AD-A161 091	
4. TITLE (and Subtitle)		5. TYPE OF REPORT & PERIOD COVERED
ANNUAL SUMMARY REPORT QUANTUM MONTE CARLO FOR MOLECULES		Annual Summary Report 1/1/85 through 12/31/85
7. AUTHOR(s)		6. PERFORMING ORG. REPORT NUMBER
William A. Lester, Jr. and Peter J. Reynolds		
1. PERFORMING ORGANIZATION NAME AND ADDRESS		8. CONTRACT OR GRANT NUMBER(s)
Materials and Molecular Research Division, Lawrence Berkeley Laboratory, University of California, Berkeley, California 94720		N00014-83-F-0101
1. CONTROLLING OFFICE NAME AND ADDRESS		10. PROGRAM ELEMENT, PROJECT, TASK AREA & WORK UNIT NUMBERS
Office of Naval Research, Physics Division Office (Code 412) 800 North Quincy Street, Arlington, Virginia 22217		61153N, RR011-03-OD, NR 602-011
14. MONITORING AGENCY NAME & ADDRESS (if different from Controlling Office)		12. REPORT DATE
		1 November 1985
		13. NUMBER OF PAGES
		30
		15. SECURITY CLASS. (of this report)
		Unclassified
		15a. DECLASSIFICATION/DOWNGRADING SCHEDULE
16. DISTRIBUTION STATEMENT (of this Report)		
<div style="border: 1px solid black; padding: 5px; text-align: center;"> <p>This document has been approved for public release and sale; its distribution is unlimited.</p> </div>		
17. DISTRIBUTION STATEMENT (of the abstract entered in Block 20, if different from Report)		
Approved for public release; distribution unlimited.		
18. SUPPLEMENTARY NOTES		
19. KEY WORDS (Continue on reverse side if necessary and identify by block number)		
Quantum Monte Carlo importance functions molecules reaction barrier theoretical excited states electronic structure energy derivatives Schrödinger equation molecular properties		
20. ABSTRACT (Continue on reverse side if necessary and identify by block number)		
Research progress on an alternative method to <u>ad initio</u> variational and perturbative approaches for the electronic structure of molecules is described. Progress in the report year on the evaluation of (1) molecular properties, (2) energy derivatives with respect to coordinates, and (3) excited states with the same symmetry as the ground state is described.		

THE FILE COPY

DD FORM 1 JAN 73 1473

EDITION OF 1 NOV 65 IS OBSOLETE

S/N 0102- LF-014-6601

Unclassified

SECURITY CLASSIFICATION OF THIS PAGE (When Data Entered)

85 11 12 178

OFFICE OF NAVAL RESEARCH

ANNUAL SUMMARY REPORT

for

1 January 1985 through 31 December 1985

for

Contract N00014-83-F-0101

Task No. RR011-03-0D

QUANTUM MONTE CARLO FOR MOLECULES

William A. Lester, Jr.
Peter J. Reynolds

Materials and Molecular Research Division
Lawrence Berkeley Laboratory
University of California
Berkeley, California 94720

TABLE OF CONTENTS

	Page
Description of Problem and Approach	1
Introduction	1
Past Work	2
QMC Theory	4
Progress in Current Year	7
Molecular Properties	7
Energy Derivatives	9
Excited States	10
Improved LiH	12
List of Manuscripts for Current Summary Year	14
Appendix	15
Related Work Supported by DOE	15
Trial Wave Functions	15
Electron Affinity of Fluorine	16
Parallel Computing	17
Related QMC Manuscripts Funded by DOE	18
References	19
Tables	22
Figure Captions	28
Figures	29



A-1

Annual Summary Report

"Quantum Monte Carlo for Molecules"

Principal Investigators:
William A. Lester, Jr.
Peter J. Reynolds

Materials and Molecular Research Division
Lawrence Berkeley Laboratory
University of California
Berkeley, California 94720

Description of Problem and Approach

Introduction.

Many-body problems in physics are often treated by a Monte Carlo approach [1]. The Monte Carlo method is statistical in nature. Based on the generation of "random" numbers or "coin tosses," it derives its name from a city famous for the random numbers embodied in its games of chance. Thus it is perhaps easy to imagine using the Monte Carlo method for treating inherently statistical models, or even for numerical integration [2]; it is, however, less obvious how to solve many-body problems with it. Nevertheless, many such problems are readily treated by Monte Carlo.

Of particular interest to molecular physics are the quantum mechanical Monte Carlo (or QMC) methods [3]. What we mean by QMC is a Monte Carlo procedure for solving the Schrödinger equation statistically by the simulation of an appropriate random process. The formal similarity of the Schrödinger equation with a diffusion equation allows one to calculate quantum mechanical expectation values as Monte Carlo averages over an ensemble of random walks. The

method is procedurally quite simple. As a result, QMC provides an attractive alternative to the conventional variational and perturbation-theoretic techniques used in physics and chemistry. — 15 1473

Past Work

We have applied QMC successfully to the calculation of the total energy of a number of molecular systems [4-7]. In every case we have achieved very high accuracy compared with experimentally inferred and exact results (where available), as well as *ab initio* configuration interaction calculations. In most cases, 90-100% of the correlation energy has been obtained.

In the past few years our research program has begun to make a more significant contribution [5-7] by obtaining quantities of more physical interest than total energies. For example, much of chemistry takes place predominantly in the valence electrons of a system. Thus the quantities of interest are usually small differences of large total energies. Examples of such differences include binding energies, electron affinities, reaction barriers, and level splittings. We have performed calculations for each of the above-mentioned quantities. Such calculations are a far more difficult task for Monte Carlo, since a small statistical uncertainty (e.g. of as little as 0.1%) in the separate total energies can mask the sought-after energy difference. To reduce the statistical error to the level needed by "brute force" is costly in computer time, as the standard deviation decreases only as $(CPU\ time)^{-1/2}$. Algorithmic developments, such as differential QMC [8] hold promise for reductions in variance through correlated sampling techniques. Another approach is based on the variance reduction achieved as a trial wave

function Ψ_T approaches the true eigenfunction. To take advantage of this latter approach we have developed an iterative procedure for improving Ψ_T [7]. We are currently working on an improved iterative procedure, as well as on different forms of correlation functions, and on methods of Monte Carlo optimization of the correlation parameters.

Using QMC, we have recently studied points along the reaction coordinate of the $H + H_2$ exchange reaction [6]. Particular emphasis has been placed on the saddle-point geometry, for which Liu [9] has performed the most extensive CI calculation to date. The bound for the barrier height which we obtained by QMC is 0.16 kcal/mole *below* Liu's bound, and probably lies within 0.1 kcal/mole of the exact answer. In addition, we were able to obtain these results with only single-determinant trial functions, and a basis set expansion at only the double-zeta level. The nodes (see below), which are important in determining the correct energy, prove to be quite insensitive to basis set beyond the double-zeta level.

Until recently, QMC applications have been limited to calculations of energies of ground states and lowest states of a given symmetry. As an example of the latter, we calculated the singlet-triplet splitting in methylene [7]. The two states studied are both lowest-energy states of their respective symmetries. In these studies, the accuracies obtained with QMC have been comparable to the best achieved by conventional *ab initio* methods. In section II, where we discuss progress during the current year, we include our recent effort in extending QMC to excited states of the same symmetry as the ground state. In that section, we also report on calculations of properties unrelated to the energy and of energy

gradient calculations. However, before going into detail, in what follows we describe the theoretical background of QMC.

QMC Theory

Briefly, one simulates a quantum molecular system by allowing it to evolve under the time-dependent Schrödinger equation in imaginary time. It is easy to show [4] that the use of imaginary time causes the system to approach a stationary state which is the lowest state of a given symmetry. Many properties may then be "measured" as averages over the resulting equilibrium distribution.

By writing the imaginary-time Schrödinger equation with a shift in the zero of energy as

$$\frac{\partial \Psi(\underline{R}, t)}{\partial t} = D \nabla^2 \Psi(\underline{R}, t) + [E_T - V(\underline{R})] \Psi(\underline{R}, t) , \quad (1)$$

we see that it may be interpreted as a generalized diffusion equation. The first term on the right-hand-side is the ordinary diffusion term, while the second term is a position-dependent rate (or branching) term. For an electronic system, $D = \hbar^2/2m_e$, \underline{R} is the three-N dimensional coordinate vector of the N electrons, and $V(\underline{R})$ is the Coulomb potential. Since diffusion is the continuum limit of a random walk, one may simulate Eq. (1) with the function Ψ (note, *not* Ψ^2) as the density of "walks". The walks undergo an exponential birth and death as given by the rate term. This connection between a quantum system and a random walk was first noted by Metropolis, who attributes it to Fermi [10].

The steady-state solution to Eq. (1) is the time-independent Schrödinger equation. Thus we have $\Psi(\underline{R}, t) \rightarrow \phi(\underline{R})$, where ϕ is an energy eigenstate. The

value of E_T at which the population of walkers is asymptotically constant gives the energy eigenvalue. Early calculations employing Eq. (1) in this way were done by Anderson on a number of one- to four-electron systems [11].

Unfortunately, in order to treat systems larger than two electrons, the Fermi nature of the electrons must be taken into account. The antisymmetry of the eigenfunction implies that Ψ must change sign; however, a density (e.g. of walkers) cannot be negative. To handle this, Anderson made simplifying assumptions about the positions of the nodes. His method was *ad hoc*, and not readily generalizable. Another method which imposes the antisymmetry, and at the same time provides more efficient sampling (thereby reducing the statistical "noise"), is importance sampling with an antisymmetric trial function Ψ_T (see e.g. Ref. 4). The zeroes (nodes) of Ψ_T become absorbing boundaries for the diffusion process: this maintains the antisymmetry. The additional boundary condition that Ψ vanish at the nodes of Ψ_T is the fixed-node approximation [4,12]. The magnitude of the error thus introduced depends on the quality of the *nodes* of $\Psi_T(\underline{R})$, and vanishes as Ψ_T approaches the true eigenfunction. To the extent that Ψ_T is a good approximation of the wave function, the true eigenfunction is almost certainly quite small near the nodes of Ψ_T . Thus one expects the fixed-node error to be small for reasonable choices of Ψ_T . Work on a number of systems has borne this out [4-7,13,14]. In addition, this error is variationally bounded.

To implement importance sampling and the fixed-node approximation, Eq. (1) is multiplied by Ψ_T , and rewritten in terms of the new probability density $f(\underline{R}, t) = \Psi_T(\underline{R})\Psi(\underline{R}, t)$. The resultant equation for $f(\underline{R}, t)$ may be written

$$\frac{\partial f}{\partial t} = D \nabla^2 f + [E_T - E_L(\underline{R})] f - D \nabla \cdot [f F_Q(\underline{R})] . \quad (2)$$

The local energy $E_L(\underline{R})$, and the "quantum force" $F_Q(\underline{R})$ are simple functions of Ψ_T given by

$$E_L(\underline{R}) \equiv H \Psi_T(\underline{R}) / \Psi_T(\underline{R}) , \quad (3a)$$

and

$$F_Q(\underline{R}) \equiv 2 \nabla \Psi_T(\underline{R}) / \Psi_T(\underline{R}) . \quad (3b)$$

Equation (2), like Eq. (1), is a generalized diffusion equation, though now with the addition of a drift term due to the presence of F_Q .

In order to perform the random walk implied by Eq. (2) we use a short-time approximation to the Green's function. The Green's function is used to evolve the distribution forward in time, i.e. $f(\underline{R}, t) \rightarrow f(\underline{R}', t + \tau)$. This process is iterated to large t . Such an approach becomes exact in the limit of vanishing time-step size, τ . Asymptotically, $f(\underline{R}, t) \rightarrow f_\infty(\underline{R}) = \Psi_T(\underline{R}) \hat{\phi}(\underline{R})$.

The function $\hat{\phi}(\underline{R})$ is the lowest-energy eigenfunction of the Schrödinger equation for the imposed set of nodes. Although neither this function nor f_∞ is known analytically, we can nevertheless sample desired quantities from the equilibrium distribution. Averages taken with respect to the distribution f_∞ are known as mixed averages. For example, sampling a quantity A in equilibrium after N samples gives the average (in the limit of large N)

$$\begin{aligned} \frac{1}{N} \sum_{configs} A &= \langle A \rangle_{f_\infty} \\ &\equiv \int f_\infty(\underline{R}) A \, d\underline{R} \end{aligned} \quad (4)$$

$$= \frac{\int \Psi_T(\underline{R}) \hat{\phi}(\underline{R}) A d\underline{R}}{\int \Psi_T(\underline{R}) \hat{\phi}(\underline{R}) d\underline{R}},$$

or in abbreviated Dirac notation (with the normalization absorbed),

$$\langle A \rangle_{f_\infty} = \langle \Psi_T | A | \hat{\phi} \rangle. \quad (5)$$

On the other hand, the correct expectation value of A , for a state $\hat{\phi}$, is $\langle \hat{\phi} | A | \hat{\phi} \rangle$. In computing the energy, or any property for which $\hat{\phi}$ is an eigenstate, there is no difference between these two averages. This follows since the eigenvalue can be taken out of the integral in the numerator of Eq. 4. In particular, to compute the energy one samples the local energy $E_L(\underline{R})$. Then

$$\begin{aligned} \langle E \rangle &= \frac{\int \hat{\phi}(\underline{R}) \Psi_T(\underline{R}) [\Psi_T^{-1}(\underline{R}) H \Psi_T(\underline{R})] d\underline{R}}{\int \hat{\phi}(\underline{R}) \Psi_T(\underline{R}) d\underline{R}} \\ &= \langle \hat{\phi} | H | \Psi_T \rangle = \hat{E}_0, \end{aligned} \quad (6)$$

where \hat{E}_0 is the eigenvalue corresponding to the state $\hat{\phi}$. The last equality follows upon noting that H is Hermitian, and thus can operate to the left. This ends our overview of QMC theory.

Progress in Current Year

Molecular Properties. For expectation values of quantities whose operators do not commute with H , the mixed average of Eq. 5 is only approximate. One suspects that the mixed average is in some sense "half-way" between the exact expectation value (with respect to $\hat{\phi}$) and the variational expectation value, taken with respect to the trial wave function, i.e. $\langle \Psi_T | A | \Psi_T \rangle$. Taken literally, this implies that $\langle \hat{\phi} | A | \hat{\phi} \rangle = 2\langle \Psi_T | A | \hat{\phi} \rangle - \langle \Psi_T | A | \Psi_T \rangle$. This result can be formalized through the following argument. The trial function

Ψ_T , if it is good, differs from $\hat{\phi}$ only by a "small" function Δ , i.e. $\hat{\phi} = \Psi_T + \Delta$.

Then

$$\begin{aligned} \langle \hat{\phi} | A | \hat{\phi} \rangle &= \langle \Psi_T | A | \hat{\phi} \rangle + \langle \Delta | A | \hat{\phi} \rangle \\ &\approx \langle \Psi_T | A | \hat{\phi} \rangle + \langle \Delta | A | \Psi_T \rangle \\ &= 2\langle \Psi_T | A | \hat{\phi} \rangle - \langle \Psi_T | A | \Psi_T \rangle. \end{aligned} \quad (7)$$

The first equality follows on expanding the $\hat{\phi}$ bra. The approximation in the next line occurs on expanding the $\hat{\phi}$ ket in the second term, and dropping the resulting term of order Δ^2 . Finally, Δ is re-expanded; A is assumed an observable, and hence Hermitian. This gives an approximate formula for expectation values taken solely with respect to $\hat{\phi}$ from just mixed and variational averages. The above argument ignores the different normalizations implicit in the different terms. However, it is easy to demonstrate that Eq. 7 divided by $\langle \hat{\phi} | \hat{\phi} \rangle$ differs from $2\langle \Psi_T | A | \hat{\phi} \rangle / \langle \Psi_T | \hat{\phi} \rangle - \langle \Psi_T | A | \Psi_T \rangle / \langle \Psi_T | \Psi_T \rangle$ by terms of only $O(\Delta^2)$. This gives the desired result. It is, however, difficult to know how significant it is to drop terms of order Δ^2 . Thus, it is desirable to be able to sample exactly from the distribution $|\hat{\phi}|^2$. This can be done, though with some changes to the usual QMC algorithm. The distribution f_∞ must be weighted locally by $\hat{\phi}(\underline{R})/\Psi_T(\underline{R})$. This quantity is essentially the asymptotic number of survivors of the local configuration \underline{R} [15]. Thus, algorithmically, one must follow each configuration into the future before computing any averages. Details of our algorithm will be presented in [16]. Our results (see Tables 1 and 2) show that while the variational approximation is poor, the approximate formula (Eq. 7) is quite good. Furthermore, excellent agreement with exact results is obtained by sampling from the pure $|\hat{\phi}|^2$ distribution.

Energy Derivatives. While conventional *ab initio* approaches regularly compute the analytic gradient of the energy with respect to nuclear coordinates in order to determine forces, and thereby equilibrium geometries [17] and (by finite difference or higher analytic derivatives) harmonic vibrational frequencies [18], only finite-difference approaches have been implemented in QMC [8]. In principle there is no reason for this limitation. To compute the energy derivative with respect to a nuclear coordinate ρ , we write

$$\begin{aligned}
 \frac{d \langle E \rangle_{f_\infty}}{d \rho} &= \frac{d}{d \rho} \left\{ \frac{\int \hat{\phi}(\underline{R}) \Psi_T(\underline{R}) E_L(\underline{R}) d\underline{R}}{\int \hat{\phi}(\underline{R}) \Psi_T(\underline{R}) d\underline{R}} \right\} \\
 &= \left\langle \frac{\partial E_L}{\partial \rho} \right\rangle_{f_\infty} \\
 &+ \left\langle \frac{1}{\hat{\phi}} \frac{\partial \hat{\phi}}{\partial \rho} E_L \right\rangle_{f_\infty} - \left\langle \frac{1}{\hat{\phi}} \frac{\partial \hat{\phi}}{\partial \rho} \right\rangle_{f_\infty} \langle E_L \rangle_{f_\infty} \\
 &+ \left\langle \frac{1}{\Psi_T} \frac{\partial \Psi_T}{\partial \rho} E_L \right\rangle_{f_\infty} - \left\langle \frac{1}{\Psi_T} \frac{\partial \Psi_T}{\partial \rho} \right\rangle_{f_\infty} \langle E_L \rangle_{f_\infty}. \tag{8}
 \end{aligned}$$

The second equality is obtained from differentiation using the chain rule, followed by expression of the resulting ratios as averages over the distribution f_∞ . The derivative $\partial \hat{\phi} / \partial \rho$ is unknown; it is however possible to sample it. The other terms in Eq. 8 may be evaluated straight-forwardly during the QMC simulation. Rather than sampling $\partial \hat{\phi} / \partial \rho$, as a first approximation we may take $\hat{\phi}^{-1} \partial \hat{\phi} / \partial \rho = \Psi_T^{-1} \partial \Psi_T / \partial \rho$. This turns out to be a good approximation even when

Ψ_T is only of moderate accuracy (e.g. double-zeta Hartree-Fock).

Using this approach, we have performed calculations on H_2 at a few nuclear separations [19]. Our results are presented in Table 3, and Figures 1 and 2, where they are compared with the essentially exact work of Kolos and Wolniewicz [20], as well as with the results of conventional *ab initio* approaches. As can be seen, QMC is competitive with CI, and far superior to Hartree-Fock. Attempting to construct the potential-energy curve of H_2 from just the four QMC energy data points (all of which are exact to within the standard error) leads to the curves of Figure 1. However, the additional information present in the first derivatives leads to a Monte Carlo potential-energy curve (cf. Fig. 2) indistinguishable from the exact one [20].

Excited States. As mentioned in Sect. I, work thus far with QMC has been limited to ground-state potential-energy surfaces and lowest-energy states of a particular symmetry [4-7,14]. For example, we have calculated the energy of the first excited state of methylene [7] in order to obtain the (until recently) elusive singlet-triplet splitting. This was the first molecular QMC calculation of an excited state. Our results there were in excellent agreement with the most recent experiments. The restriction on lowest energy states of a symmetry comes from an essential feature of the mapping of the Schrödinger equation into its diffusion analog--namely, that time in these two equations differs by a factor of i . This means that the expansion of a time-dependent molecular state vector in energy eigenfunctions multiplied by $\exp(-iEt/\hbar)$, results in a series in which only the lowest energy term (i.e. $\hat{\phi}$) survives at large t . Thus one obtains exponential

convergence to the lowest energy eigenstate.

If Ψ_T is orthogonal to the exact lowest-energy state, one can see from Eq. 6 that convergence will be to the next-lowest energy. (Initially $\hat{\phi}$ contains a superposition of states.) This fact actually is used even in the calculation of molecular ground-state energies, as Fermi states are excited states (with respect to the Boson ground state) of the Schrödinger equation. By choosing Ψ_T to be antisymmetric with respect to particle exchange, one can project out all symmetric states. A similar result holds for calculations of different symmetry states of a given molecule.

When studying states of the same symmetry, it is generally not possible to find a trial wave function exactly orthogonal to all the lower-energy states of that symmetry. This implies that convergence will ultimately be to the lowest-energy state. However, the fixed-node approximation used to treat the Fermi problem is of assistance here too. In the fixed-node approximation, the nodes of Ψ_T are used to divide \underline{R} -space into separate volume elements. The Schrödinger equation is solved separately in each of these elements. This results in a solution of the Schrödinger equation with added boundary conditions. Viewed this way, the Fermi problem is handled by forcing the generation of an antisymmetric state above the Bose ground state through the placement of nodes in the solution $\hat{\phi}$. In like manner, other excited states can be treated approximately by imposing additional nodes. The accuracy of the approximation will depend on how well these nodes are placed.

In treating excited states, traditional *ab initio* methods generate wave functions with the correct number and dimensionality of nodes. Thus such wave functions are a good place to begin in searching for an excited-state Ψ_T . We report preliminary results achieved with QMC in this way. A more detailed report is in preparation [21]. Tables 4 and 5 report our results on respectively the first two excited state of the He atom (which are of the same symmetry as the ground state) and of the first excited state of H_2 (which is of a different symmetry than the ground state). In the case of He, we have obtained 64% of the correlation energy for the $1s2s\ ^1S$ state and 90% of the correlation energy of the $1s3s\ ^1S$ state. Though the former appears low (percentage-wise), we note that our total energy is within 0.66 kcal/mol of the experimental energy, which is generally regarded as chemical accuracy. For H_2 we note that there is some basis-set dependence--at least with such small bases. Nevertheless, a fairly simple basis set (double-zeta plus polarization) yields approximately 80% of the correlation energy. We expect that better results will be obtained through the use of better optimized trial functions.

Improved LiH. In test runs on our properties and derivatives programs, as well as in tests on our new correlation functions [see (1) in Appendix], we have been using the LiH molecule as a sample system. In the course of these runs, we have calculated new bounds on the ground-state energy of LiH. In fact, our new correlation function has allowed us to rapidly reduce our variance for this energy. Our previous LiH results [4] were better than any *ab initio* calculations available at the time. Recently, workers using CI techniques have put a large effort into

showing that "they could do better than QMC." They achieved a new energy bound, lower than our old QMC results. However, as a result of our test runs alone, we have achieved an energy which is essentially the exact result (Table 6).

List of Manuscripts for Current Summary Year

1. "Quantum Monte Carlo Calculation of the Singlet-Triplet Splitting in Methylene" P. J. Reynolds, M. Dupuis, and W. A. Lester, Jr., J. Chem. Phys. 82, 1983 (1985). (Jointly supported by DOE.)
2. "H + H₂ Reaction Barrier: A Quantum Monte Carlo Study" R. N. Barnett, P. J. Reynolds, and W. A. Lester, Jr., J. Chem. Phys. 82, 2700 (1985). (Jointly supported by DOE.)
3. "Quantum Chemistry by Quantum Monte Carlo: Beyond Ground-State Energy Calculations" P. J. Reynolds, R. N. Barnett, B. L. Hammond, R. M. Grimes, and W. A. Lester, Jr., Int. J. Quant. Chem. *accepted*
4. "Molecular Physics Applications of Quantum Monte Carlo" P. J. Reynolds, R. N. Barnett, B. L. Hammond, R. M. Grimes, and W. A. Lester, Jr., J. Stat. Phys. *to appear*.
5. "Molecular Properties by Quantum Monte Carlo" R. N. Barnett, P. J. Reynolds, and W. A. Lester, Jr., *in preparation*.
6. "Molecular Excited States with Fixed-Node Quantum Monte Carlo" R. M. Grimes, R. N. Barnett, P. J. Reynolds, and W. A. Lester, Jr., *in preparation*.
7. "Energy Derivatives by Quantum Monte Carlo" B. L. Hammond, P. J. Reynolds, and W. A. Lester, Jr., *in preparation*.

Appendix

Related Work Supported by DOE

Trial Wave Functions. For use in QMC one wants a trial function which is as simple as possible, since it will require repeated evaluation at each step of the random walk. Yet one wants a function which provides accurate results. In principle, since QMC solves the Schrödinger equation, one should obtain accurate results *regardless* of the choice of Ψ_T . However, as we noted already, for Fermi systems inaccurate nodes in Ψ_T will lead to a small error when the fixed-node approximation is used. Furthermore, the statistical "noise" will be large for a poor choice of Ψ_T .

We have found in our work that a *single determinant* Ψ_T with only a double-zeta basis set places the nodes extremely well in ground-state calculations, as determined by the quality of the computed total energies. Increasing the basis set beyond double zeta appears to offer insignificant gain in either accuracy (i.e. the fixed-node error does not noticeably decrease) or precision (the statistical uncertainty, for equal computing time, remains essentially unchanged). In practice we have included an electron-electron Jastrow factor in our functions Ψ_T in order to reduce statistical fluctuations, and in many cases we have also included an electron-nuclear factor. Neither factor affects the positioning of the nodes, and hence the fixed-node energies remain unchanged. However, the Jastrow's do have an important effect on variance reduction.

By optimization of a small number of parameters (2 - 4), it appears that an order of magnitude improvement in computer time can be achieved. Additionally, we are now experimenting with other forms of correlation function in the hope of finding further variance reduction. In contrast to the usual Jastrow forms of

$$J_{ij} = \exp \left\{ \sum_{ij} \frac{ar_{ij}}{1+br_{ij}} \right\}, \quad (\text{A1a})$$

and

$$J_{i\alpha} = \exp \left\{ \sum_{i\alpha} \frac{\lambda r_{i\alpha}}{1+\nu r_{i\alpha}} \right\}, \quad (\text{A1b})$$

for the electron-electron and electron-nuclear terms respectively, we have done some experimentation with an electron-electron correlation function of the form

$$\prod_{ij} (1 - a \exp(br_{ij} + cr_{ij}^d)). \quad (\text{A2})$$

A similar form can be used for the electron-nuclear correlation function. As with the Jastrow form, only the variance is affected, as this term does not introduce any nodes of its own. It turns out that this form is considerably more flexible than Eq. (A1). Although an extended Jastrow form appears to offer the same flexibility, it appears more difficult to optimize. Iterative improvement of Ψ_T is also of potential benefit. One such scheme--a global rescaling of Ψ_T --has been described by us [7]. A more powerful, local scheme is being developed currently.

Electron Affinity of Fluorine. Although properties for which $\hat{\phi}$ is not an eigenstate, such as the electronic charge distribution, need to be sampled as described in point (1) above, many important quantities are energy related.

These quantities can be computed more simply--though two different energies must be calculated very accurately. One such energy-related quantity is the electron affinity. This past year we have performed an accurate QMC calculation of the electron affinity of fluorine [22]. These results--like our energies--exceed the quality of the best variational calculations, and are in excellent accord with the recommended experimental value.

Parallel Computing. Monte Carlo, as alluded to earlier, is such a computationally intensive activity that new techniques are needed if one wishes to attack large systems or obtain very high precision (e.g. better than 99.99%). One avenue we have explored, in collaboration with the Advanced Computer Architecture Laboratory at LBL, is the use of parallel computing architectures [23]. Briefly, we have found that Monte Carlo can be readily made to run at 95% efficiency on an 8 processor system. We explored several different directions for parallelizing QMC, as well as load-balancing techniques to keep the efficiency near 100%. It is expected that a slightly restructured parallel code can run at essentially 100% efficiency with an almost unlimited number of processors. Thus, with sufficient memory, precision will scale as the square root of the number of processors, while computing time for a fixed precision will scale inversely almost linearly with processors.

Related QMC Manuscripts funded by DOE

1. "Exact Monte Carlo for Molecules" W. A. Lester, Jr. and P. J. Reynolds
Proceedings of the Florida A & M University Spring Science Seminars
March 28-29, 1985.
2. "Vector and Parallel Computers for Quantum Monte Carlo Computations"
P. J. Reynolds, S. Alexander, D. Logan, and W. A. Lester, Jr.,
in *Lecture Notes in Chemistry*, E. Clementi and M. Dupuis, eds. (Springer-
Verlag, Berlin 1986).
3. "Vectorization of Molecular Quantum Monte Carlo" S. Alexander, P. J.
Reynolds, R. N. Barnett, and W. A. Lester, Jr. *in preparation*.
4. "Parallelism in Quantum Monte Carlo: Calculation of the Binding Energy
of the Nitrogen Molecule" P. J. Reynolds, D. Logan, C. Maples, and
W. A. Lester, Jr. *in preparation*.
5. "Electron Affinity of Fluorine: Quantum Monte Carlo Study" R. N.
Barnett, P. J. Reynolds, and W. A. Lester, Jr., *J. Chem. Phys.*
in preparation.

References

- [1] See, e.g., *Monte Carlo Methods in Statistical Physics*, K. Binder, ed. (Springer-Verlag, Berlin, 1979).
- [2] J. M. Hammersley and D. C. Handscomb, *Monte Carlo Methods*, (Chapman and Hall, London, 1964).
- [3] M. H. Kalos, Phys. Rev. 128, 1791 (1962); J. Comp. Phys. 1, 257 (1967); M. H. Kalos, D. Levesque, and L. Verlet, Phys. Rev. A 9, 2178 (1974); D. M. Ceperley in *Recent Progress in Many-Body Theories*, edited by J. G. Zabolitzky, M. de Llano, M. Fortes, and J. W. Clark (Springer-Verlag, Berlin, 1981); D. M. Ceperley and M. H. Kalos in Ref. [1].
- [4] P. J. Reynolds, D. M. Ceperley, B. J. Alder, and W. A. Lester, Jr., J. Chem. Phys. 77, 5593 (1982).
- [5] P. J. Reynolds, R. N. Barnett, and W. A. Lester, Jr., Int. J. Quant. Chem. Symp. 18, 709 (1984).
- [6] R. N. Barnett, P. J. Reynolds, and W. A. Lester, Jr., J. Chem. Phys., 82, 2700 (1985).
- [7] P. J. Reynolds, M. Dupuis, and W. A. Lester, Jr., J. Chem. Phys. 82, 1983 (1985).
- [8] B. Holmer and D. M. Ceperley, *private communication*; B. Wells, P. J. Reynolds, and W. A. Lester, Jr., *unpublished*; B. H. Wells, Chem. Phys. Lett. 115, 89 (1985).
- [9] B. Liu, J. Chem. Phys. 80, 581 (1984).
- [10] N. Metropolis and S. M. Ulam, J. Am. Stat. Assoc. 44, 335 (1949).
- [11] J. B. Anderson, J. Chem. Phys. 63, 1499 (1975); 65, 4121 (1976).
- [12] D. M. Ceperley and B. J. Alder, Phys. Rev. Lett. 45, 566 (1980).
- [13] J. B. Anderson, J. Chem. Phys. 73, 3897 (1980); F. Mentch and J. B. Anderson, J. Chem. Phys. 74, 6307 (1981).
- [14] J. W. Moskowitz, K. E. Schmidt, M. A. Lee, and M. H. Kalos, J. Chem. Phys. 77, 349 (1982).

- [15] M. H. Kalos, Phys. Rev. A 2, 250 (1970).
- [16] R. N. Barnett, P. J. Reynolds, and W. A. Lester, Jr., "Molecular Properties by Quantum Monte Carlo" *in preparation*.
- [17] P. Pulay, in *Modern Theoretical Chemistry*, Vol. 4, H. F. Schaefer III, ed. (Plenum, New York, 1977); M. Dupuis and H. F. King, J. Chem. Phys. 68, 3998 (1978).
- [18] P. Saxe, Y. Yamaguchi, and H. F. Schaefer III, J. Chem. Phys. 77, 5647 (1982).
- [19] B. L. Hammond, P. J. Reynolds, and W. A. Lester, Jr., "Energy Derivatives by Quantum Monte Carlo", *in preparation*.
- [20] W. Kolos and L. Wolniewicz, J. Chem. Phys. 43, 2429 (1965).
- [21] R. N. Grimes, R. N. Barnett, P. J. Reynolds, and W. A. Lester, Jr., "Molecular Excited States with Fixed-Node Quantum Monte Carlo" *in preparation*.
- [22] R. N. Barnett, P. J. Reynolds, and W. A. Lester, Jr., "Electron Affinity of Fluorine: Quantum Monte Carlo Study" J. Chem. Phys. *submitted*.
- [23] P. J. Reynolds, S. Alexander, D. Logan, and W. A. Lester, Jr., "Vector and Parallel Computers for Quantum Monte Carlo Computations", to appear in *Lecture Notes in Chemistry* (Springer-Verlag, Berlin); P. J. Reynolds, D. Logan, C. Maples, and W. A. Lester, Jr., "Parallelism in Quantum Monte Carlo: Calculation of the Binding Energy of the Nitrogen Molecule" *in preparation*.
- [24] A. D. Mc Lean and M. Yoshimine, J. Chem. Phys. 45, 3676 (1966).
- [25] W. Kolos and L. Wolniewicz, J. Chem. Phys. 41, 3674 (1963).
- [26] F. Billingsley and M. Krauss, J. Chem. Phys. 60, 2767 (1974).
- [27] D. E. Stogryn and A. P. Stogryn, Mol. Phys. 11, 371 (1966). See also Table 2 in Ref. [17].
- [28] W. Kolos and C. C. J. Roothaan, Rev. Mod. Phys. 32, 219 (1960).
- [29] B. Liu, J. Chem. Phys. 58, 1925 (1973).
- [30] Z. Ritter and R. Pauncz, J. Chem. Phys. 32, 1820 (1960).

- [31] C. E. Moore, Natl. Bur. Standards Circ. No. 467, I (1948).
- [32] R. Grimes, M. Dupuis, and W. A. Lester, Jr., *unpublished results*.
- [33] R. Grimes, M. Dupuis and W. A. Lester, Jr., Chem. Phys. Lett. 110, 247 (1984).
- [34] W. Kolos and L. Wolniewicz, J. Chem. Phys. 49, 404 (1968).
- [35] W. Meyer and P. Rosmus, J. Chem. Phys. 63, 2356 (1975).
- [36] N. C. Handy, R. J. Harrison, P. J. Knowles, and H. F. Schaefer III, J. Phys. Chem. 88, 4852 (1984).
- [37] L. Wharton, L. Gold, and W. Klemperer, J. Chem. Phys. 37, 2149 (1962).

Table 1. Comparison of expectation values for properties of H_2 . The properties studied are expectation values of the squared distance from the H_2 axis, along the H_2 axis, and from the center of the molecule (in bohr²). The electric quadrupole moment, Q , (in esu·cm²×10⁻²⁶) can be derived from the other expectation values. The trial function, Ψ_T , is a single-zeta-plus-bond SCF function, multiplied by electron-electron and electron-nuclear Jastrow functions. The function, $\hat{\phi}$, is the exact wave function in this case, since there are no nodes for the ground-state of H_2 . However, a small bias due to the short-time approximation may be present. Here the time step is $\tau=0.01$ au. "Approximate formula" refers to Eq. 7 of the text. Statistical uncertainty in the last significant figures is shown in parentheses.

Method	$(\langle x^2 \rangle + \langle y^2 \rangle)$	$\langle z^2 \rangle$	$\langle r^2 \rangle$	Q
Best Variational ^a	1.554	1.020	2.574	0.664
$\langle \Psi_T A \Psi_T \rangle$	1.543(2)	1.078(2)	2.621(3)	0.49(1)
$\langle \Psi_T A \hat{\phi} \rangle$	1.534(5)	1.047(4)	2.580(9)	0.56(2)
Approximate Formula	1.525(10)	1.016(9)	2.539(18)	0.63(5)
$\langle \hat{\phi} A \hat{\phi} \rangle$	1.527(6)	1.025(5)	2.552(10)	0.61(3)
Exact ^b	1.523	1.023	2.546	0.61

^a Ref. 24.

^b Ref. 25.

Table 2. Comparison of values obtained for the electric quadrupole moment of N_2 . The trial function, Ψ_T , is a double-zeta SCF function, multiplied by electron-electron and electron-nuclear Jastrow functions. Time steps of $\tau=0.0025$ and 0.00125 au are used, with no noticeable bias present. "Approximate formula" refers to Eq. 7 of the text. Statistical uncertainties are indicated in parentheses.

Method	Q (esu·cm ² ×10 ⁻²⁶)
Hartree-Fock ^a	-1.29
MCSCF ^a	-1.22
$\langle \Psi_T Q \Psi_T \rangle$	-2.19(4)
$\langle \Psi_T Q \hat{o} \rangle$	-1.80(10)
Approximate Formula	-1.41(20)
Experiment ^b	-1.4(1)

^a Ref. 26.

^b Ref. 27.

Table 3. Comparison of energy derivatives of H_2 at various geometries with standard techniques. The QMC trial function consists of a double-zeta SCF wave function multiplied by an electron-electron correlation function of the form $\prod_{ij}(1-a \exp(br_{ij}+cr_{ij}^d))$. The parameters used are $a=0.48$, $b=0.54$, $c=0.33$, and $d=1.4$. Time steps ranging from $\tau=0.1$ au to $\tau=0.005$ au are used. The quoted results are extrapolations to $\tau=0$. Energies are in hartrees and derivatives in hartrees/bohr. Statistical uncertainties are indicated in parentheses.

Method	$\rho=0.4$ bohr		$\rho=0.9$ bohr		$\rho=1.4011$ bohr		$\rho=1.9$ bohr	
	E	$dE/d\rho$	E	$dE/d\rho$	E	$dE/d\rho$	E	$dE/d\rho$
SCF	-0.0787 ^a	-5.030 ^a	-1.0433 ^a	-0.5145 ^a	-1.1335 ^b	0.0053 ^b	-1.1017 ^a	0.0970 ^a
CI ^c	---	---	-1.0826	-0.5101	-1.1737	0.0007	-1.1461	0.0851
QMC ^d	-0.1192(13)	-5.297(12)	-1.0831(12)	-0.5053(45)	-1.1745(12)	0.0009(24)	-1.1467(11)	0.1028(55)
Exact ^e	-0.1202	-5.307	-1.0836	-0.5007	-1.1745	0.0000	-1.1469	0.0852

^a Ref. 28.

^b Pulay in Ref. 17.

^c Ref. 29.

^d Present work.

^e Ref. 20.

Table 4. Comparison of the energy of the first two excited 1S states of He with SCF and experiment. The SCF wave function, whose energy is shown in the table, is used as the QMC Ψ_T . The column headed %CE gives the percentage of the correlation energy recovered, and is computed relative to the SCF number in the first row of the table. A time step of $\tau=0.05$ au is used. Statistical uncertainties are indicated in parentheses.

Method	1s2s			1s3s		
	$E_1(h)$	%CE	$\Delta(E - E_{\text{exp}})$ (kcal/mole)	$E_2(h)$	%CE	$\Delta(E - E_{\text{exp}})$ (kcal/mol)
SCF ^a	-2.14307	0	1.83	-2.06036	0	0.577
QMC	-2.14493(7)	64	0.66(4)	-2.06119(7)	90	0.06(4)
Experiment ^b	-2.14598	100	0.00	-2.06128	100	0.00

^a Ref. 30.

^b Ref. 31.

Table 5. Comparison of the energy of the first excited singlet state of H_2 ($B^1\Sigma_u^+$) at its equilibrium geometry with self-consistent field (SCF), configuration interaction (CI) and exact results. For QMC, two different trial functions are used. They are constructed from double-zeta (DZ) and double-zeta-plus-polarization (DZP) SCF functions. The column headed % CE gives the percentage of correlation energy recovered, and is computed relative to the SCF number in the first row of the table. A time step of $\tau=0.01$ au is used. Statistical uncertainties are indicated in parentheses.

Method	$E(h)$	% CE	$\Delta(E-E_{exact})$ (kcal/mole)
SCF	-0.742 ^a	0	9.4
QMC (DZ)	-0.748(2)	41	5.6
QMC (DZP)	-0.7536(3)	79	1.9
CI	-0.7553 ^b	90	0.9
Exact	-0.7567 ^c	100	0.0

^a Ref. 32.

^b Ref. 33.

^c Ref. 34.

Table 6. Comparison of LiH energies (in hartrees).

Method	E
Best variational ^a (pre-1982)	-8.065
QMC (1982) ^b	-8.067(2)
CI (current) ^c	-8.0690
QMC (current)	8.0702(4)
"Exact" ^d	8.0705

^a Ref. 35^b Ref. 4^c Ref. 36^d Ref. 37

Figure Captions

Figure 1. Fit of the potential energy curve for H_2 . Two different fits to the four energy points are shown. Neither a third-order Legendre polynomial fit, nor an exponential spline, gives an adequate representation of the curve compared with the exact potential of Kolos and Wolniewicz.

Figure 2. Fit of the potential energy curve for H_2 including energy derivatives. A Hermite polynomial fit to the data, which is possible with the additional information available from the derivatives, is indistinguishable from the exact curve.

Hydrogen Molecule Potential Curve

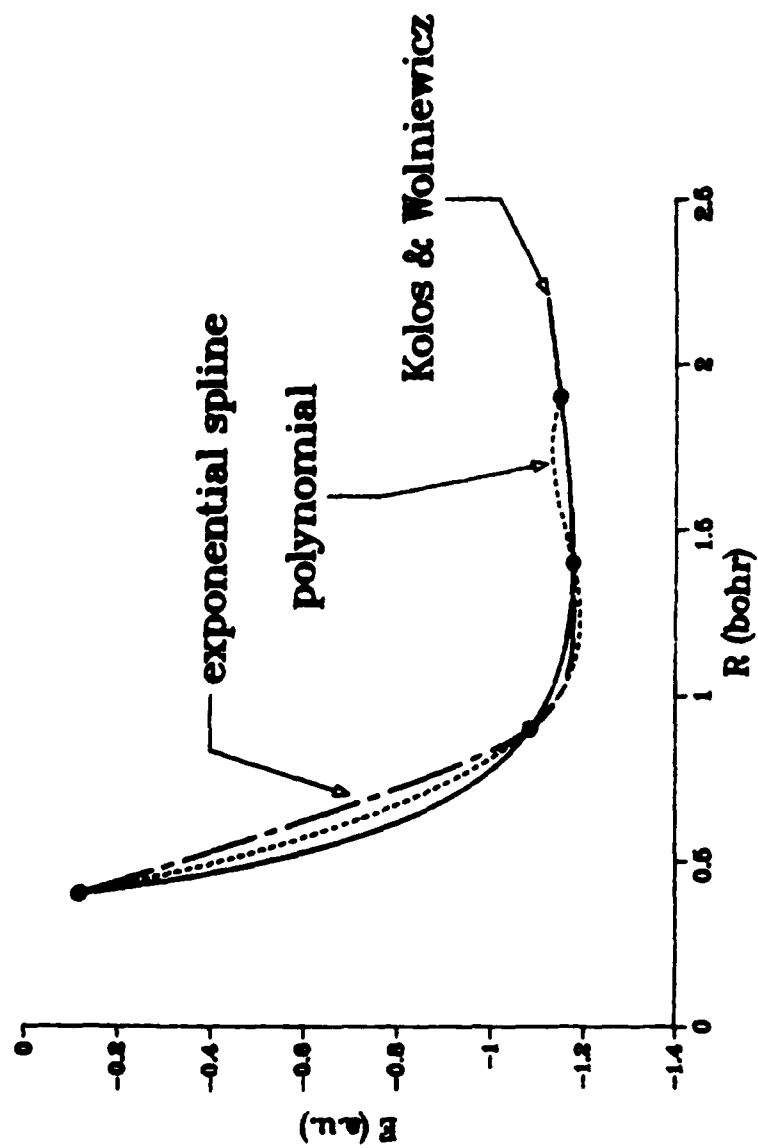


Figure 1.

Hydrogen Molecule Potential Curve

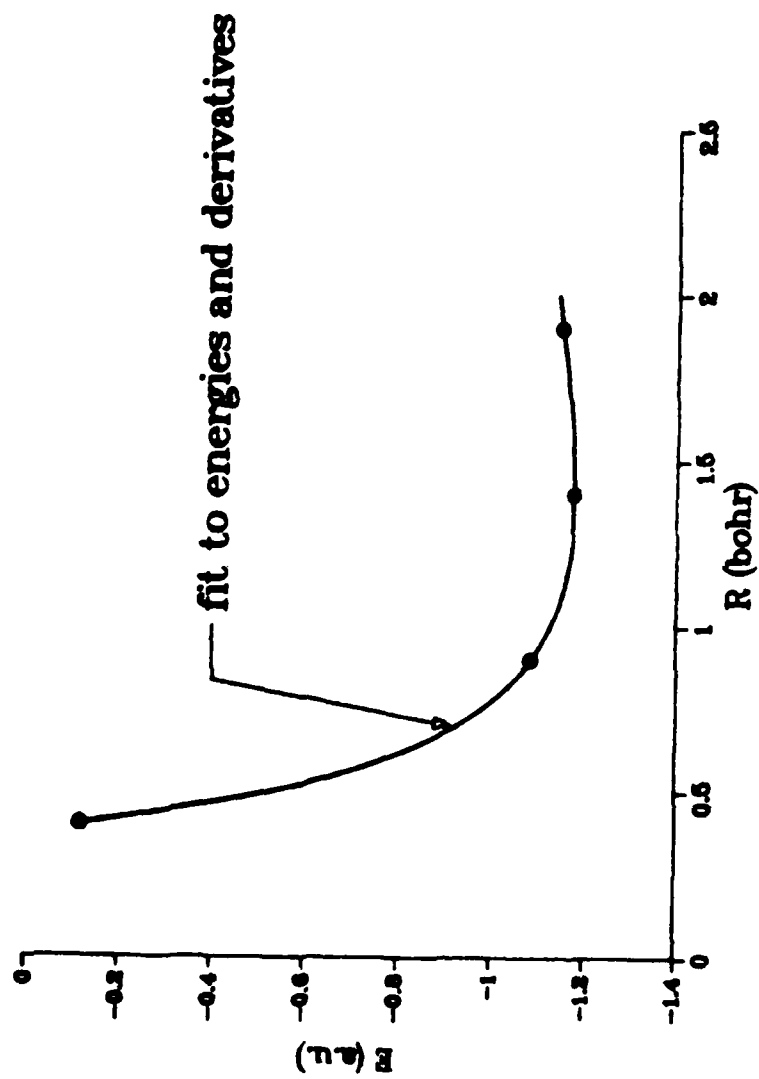


Figure 2.

END

FILMED

12-85

DTIC